ENVIRONMENTAL RESEARCH
LETTERS

LETTER • OPEN ACCESS

Aboveground carbon loss associated with the spread of ghost forests as sea levels rise

To cite this article: Lindsey S Smart *et al* 2020 *Environ. Res. Lett.* **15** 104028

Environmental Research Letters

LETTER

Aboveground carbon loss associated with the spread of ghost forests as sea levels rise

Lindsey S Smart[1], Paul J Taillie[2], Benjamin Poulter[3], Jelena Vukomanovic[1,4], Kunwar K Singh[5,6], Jennifer J Swenson[7], Helena Mitasova[1,8], Jordan W Smith[9] and Ross K Meentemeyer[1,10]

[1] Center for Geospatial Analytics, North Carolina State University, 2800 Faucette Drive, Raleigh, NC 27695, United States of America
[2] Department of Wildlife Ecology and Conservation, University of Florida, Gainesville, FL 32611, United States of America
[3] Biospheric Sciences Laboratory, NASA Goddard Space Flight Center, Greenbelt, MD 20771, United States of America
[4] Department of Parks, Recreation, and Tourism Management, North Carolina State University, 2800 Faucette Drive, Raleigh, NC 27695, United States of America
[5] The Institute for Global Research, AidData, The College of William and Mary, 424 Scotland Street, Williamsburg, VA, 23185, United States of America
[6] Center for Geospatial Analysis, The College of William and Mary, 400 Landrum Drive, Williamsburg, VA, 23185, United States of America
[7] Nicholas School of the Environment, Duke University, 9 Circuit Drive, Durham, NC 27710, United States of America
[8] Department of Marine, Earth and Atmospheric Sciences, North Carolina State University, 2800 Faucette Drive, Raleigh, NC 27695, United States of America
[9] Department of Environment and Society, Utah State University, 5215 Old Main Hill, Logan, UT 84322, United States of America
[10] Department of Forestry and Environmental Resources, North Carolina State University, 2800 Faucette Drive, Raleigh, NC 27695, United States of America

E-mail: lssmart@ncsu.edu

Keywords: ghost forests, sea level rise, saltwater intrusion, LiDAR, aboveground carbon

Supplementary material for this article is available online

OPEN ACCESS

RECEIVED
24 February 2020

REVISED
18 June 2020

ACCEPTED FOR PUBLICATION
30 June 2020

PUBLISHED
22 September 2020

Abstract

Coastal forests sequester and store more carbon than their terrestrial counterparts but are at greater risk of conversion due to sea level rise. Saltwater intrusion from sea level rise converts freshwater-dependent coastal forests to more salt-tolerant marshes, leaving 'ghost forests' of standing dead trees behind. Although recent research has investigated the drivers and rates of coastal forest decline, the associated changes in carbon storage across large extents have not been quantified. We mapped ghost forest spread across coastal North Carolina, USA, using repeat Light Detection and Ranging (LiDAR) surveys, multi-temporal satellite imagery, and field measurements of aboveground biomass to quantify changes in aboveground carbon. Between 2001 and 2014, 15% (167 km^2) of unmanaged public land in the region changed from coastal forest to transition-ghost forest characterized by salt-tolerant shrubs and herbaceous plants. Salinity and proximity to the estuarine shoreline were significant drivers of these changes. This conversion resulted in a net aboveground carbon decline of 0.13 ± 0.01 TgC. Because saltwater intrusion precedes inundation and influences vegetation condition in advance of mature tree mortality, we suggest that aboveground carbon declines can be used to detect the leading edge of sea level rise. Aboveground carbon declines along the shoreline were offset by inland aboveground carbon gains associated with natural succession and forestry activities like planting (2.46 ± 0.25 TgC net aboveground carbon across study area). Our study highlights the combined effects of saltwater intrusion and land use on aboveground carbon dynamics of temperate coastal forests in North America. By quantifying the effects of multiple interacting disturbances, our measurement and mapping methods should be applicable to other coastal landscapes experiencing saltwater intrusion. As sea level rise increases the landward extent of inundation and saltwater exposure, investigations at these large scales are requisite for effective resource allocation for climate adaptation. In this changing environment, human intervention, whether through land preservation, restoration, or reforestation, may be necessary to prevent aboveground carbon loss.

1. Introduction

Coastal forests sequester and store more carbon per unit area than upland forest (McLeod *et al* 2011; Simard *et al* 2019), storing carbon both near-term in aboveground biomass and longer-term in sediments (Duarte and Prairie 2005, Poulter *et al* 2008, Noe *et al* 2016, Krauss *et al* 2017). Despite their limited global extent, they play a disproportionately important role in the global carbon cycle (Poulter *et al* 2006; Henman and Poulter 2008). Through sequestration and storage, coastal forests provide critical ecosystem services that help regulate global climate and mitigate climate change (MEA 2005, McLeod *et al* 2011). However, these coastal systems are shrinking precipitously due to human land-use modifications and sea level rise (McLeod *et al* 2011, Pendleton *et al* 2012). As sea levels rise, inundation, saltwater intrusion, and land loss will increase (Church and White 2011, Church *et al* 2013, Dangendorf *et al* 2017), compounding the negative impacts from human pressures (He and Silliman 2019). Coastal systems have always been considered dynamic and resilient (Kirwan and Megonigal 2013), however, their ability to adapt to this rapid change is uncertain.

The freshwater-dependent plant species characteristic of temperate coastal forests have varying tolerances to inundation and salinity. Initially, exposure primarily impacts seedlings by inhibiting regeneration (Brinson *et al* 1995, Williams *et al* 1998, DeSantis *et al* 2007, Krauss *et al* 2009, Langston *et al* 2017). Mature trees can generally withstand short periods of inundation and exposure, but prolonged exposure leads to osmotic stress and eventual mortality (Kirwan *et al* 2007, Conner *et al* 2007, Krauss *et al* 2018).

In response to increased salinization and inundation, freshwater-dependent coastal forests are retreating upslope, leaving behind dead trees surrounded by salt-tolerant shrubs and herbaceous plant species (Hackney and Yelverton 1990, Williams *et al* 1999a). This conversion can occur over the course of a decade or more (Craft 2012, White and Kaplan 2017). These 'ghost forests' are common along the North Atlantic Coast and Gulf of Mexico, varying geographically in extent and conversion rates due to spatial variation in plant community composition (Poulter *et al* 2008, 2009, Kirwan and Gedan 2019) and relative sea level rise rates (Karegar *et al* 2016, 2017). Ghost forests are part of a transition zone between coastal forest and marsh (figure 1), and can remain visible on the landscape for decades after the forest has functionally transitioned to marsh (Williams *et al* 1999b, Moorman *et al* 1999), serving as late-stage indicators of saltwater intrusion.

Multi-layered and structurally complex coastal forests transition to marshes with very little complexity following saltwater intrusion. Losses in structural complexity have important implications for carbon storage. Because aboveground carbon is closely linked with plant height (Jenkins *et al* 2003), we expect that conversion from forest to marsh will decrease aboveground carbon storage. As evidenced in other biomes, the transition from forest to herbaceous plant communities (e.g. grasslands) decreases aboveground carbon storage and increases albedo, which exacerbates the effects of greenhouse gases (Gibbon *et al* 2010, Kirschbaum *et al* 2012). In coastal systems, the impacts of ghost forest proliferation on ecosystem services, particularly carbon storage, are understudied (Conner *et al* 2007, Erwin 2009, Tully *et al* 2019). The broad spatial and temporal extents at which conversion occurs make measurement particularly difficult. Making quantification even more difficult, local-scale factors such as salinity gradients, wind tides, surface water flow, and geologic activity (e.g. subsidence), create fine-scale heterogeneity across these broad extents (Ardón *et al* 2013, Herbert *et al* 2015).

We integrated multiple sources of remote sensing data and field data to quantify changes in aboveground carbon storage across a large low-lying coastal region in North Carolina, USA. Past studies examining landscape-scale changes in coastal forests have focused on tropical mangrove forests (e.g. Hamilton and Casey 2016, Thomas *et al* 2017) not freshwater-dependent temperate forests (however, see Raabe and Stumpf 2016, Schieder *et al* 2018), and have not addressed associated aboveground carbon storage dynamics (however, in mangrove forests, see Lagomasino *et al* 2019). To our knowledge, ours is the first study to examine landscape-scale aboveground carbon dynamics related to ghost forest proliferation, a phenomenon unique to temperate regions. Our objectives were to (1) map the 13-year spread of ghost forests in a large low-lying coastal region, (2) quantify the associated loss in aboveground carbon, and (3) compare forest loss from ghost forest spread to other sources of disturbance (e.g. wildfires and forestry activities). Because coastal forests serve as buffers against storm surges (Barbier *et al* 2011), provide habitat for wildlife species (Field *et al* 2016, Taillie *et al* 2019), and preserve productivity of lands in coastal communities (McNulty *et al* 2015, Tully *et al* 2019), the ability to identify landscape-scale transitions from forest to marsh is ecologically and economically important. The carbon dynamics related to this unique transition also highlight a potentially important positive feedback loop between climate change and greenhouse gas emissions (Henman and Poulter 2008). By examining spatio-temporal patterns in ghost forest extent and aboveground carbon, we demonstrate how saltwater intrusion from sea level rise impacts important carbon pools in temperate coastal forests. As sea level rise accelerates, landscape-scale measurements of this phenomenon are integral to a better understanding of the impacts of climate on the global carbon cycle and the continued persistence of critical ecosystem services.

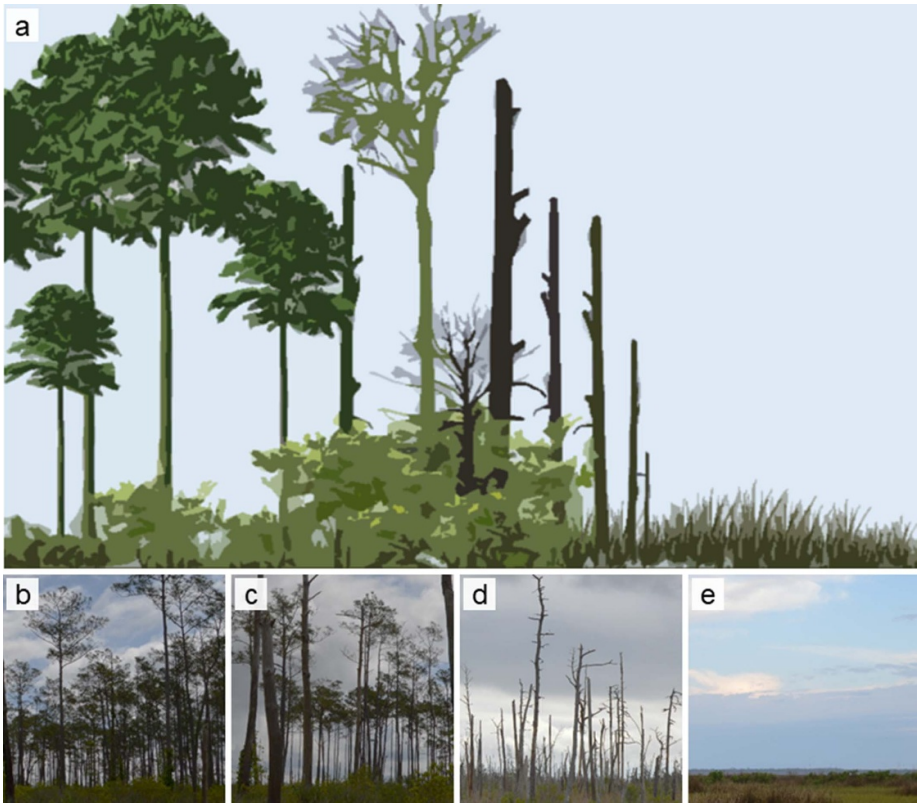

Figure 1. (a) Schematic of the forest-to-marsh transition gradient typical in eastern North Carolina, USA. (b) Coastal forests, dominated by loblolly pine (*Pinus taeda*), bald cypress (*Taxodium distichum*), or pond pine (*Pinus serotina*), give way to (c) 'transition forest' with an abundance of shrub and herbaceous species that have higher salt tolerances. (d) In later stages, marked by a greater number of dead standing trees, transition forest is generally referred to as 'ghost forest.' Without competition from tree seedlings, salt-tolerant marsh species migrate into the area (referred to as marsh migration), completing the transition to (e) herbaceous marsh comprised of brackish or saline herbaceous plant species like sawgrass (*Cladium jamaicense*) and black needlerush (*Juncus romerianus*). (Image credit: L S Smart.)

2. Methods

Our study area was an approximately 4000-km^2 portion of the Albemarle-Pamlico Peninsula in eastern North Carolina, USA, buffered from the Atlantic Ocean by a chain of barrier islands and the Albemarle and Pamlico Sounds. Almost half (47%) of the peninsula is < 1 m in elevation (figure 2(a)); the region is therefore highly vulnerable to sea level rise impacts, and saltwater intrusion has already caused forest decline here (Young 1995, Moorhead and Brinson 1995, Poulter 2005). Forty percent of the lands on the peninsula are publicly owned; most of these are 'unmanaged'. We refer to these areas as 'unmanaged' because there are no extractive activities, but they may be managed for biodiversity, which can include mimicking disturbance events (e.g. controlled or prescribed burning to imitate natural fire disturbances) and controlling water flow. Managed public lands refer to lands that are subject to extractive use (e.g. logging or mining) (figure 2(b)). Privately held lands are comprised of a mix of natural forest, agriculture, and forestry uses (figure 2(b)).

We collected field data at five sites along the shoreline of the Albemarle-Pamlico Peninsula. Each site was accessible by road, under 1 m in elevation, and publicly owned (no active management at the site). At each site, we sampled evenly across the forest-marsh gradient by delineating three vegetation zones (forest, transition-ghost forest, and marsh) using aerial photographs and confirmed these in the field as part of the sampling protocol (Poulter *et al* 2005). We randomly selected seven 12-m-radius vegetation plots in each zone (figure 2(b)). At each plot, we recorded species name, diameter at breast height (DBH), and height for live woody species greater than 2.5 cm in diameter; for vegetation less than 1 m in height, we recorded percent cover within five 1-m^2 subplots. We averaged percent cover across the five subplots to obtain an average cover value for each species. We calculated the aboveground biomass of each plant documented in the field by applying species-specific allometric equations (table S3; Smith and Brand 1983; Jenkins *et al* 2003; Castillo *et al* 2008; Trilla *et al* 2009; Riegel *et al* 2013). For each plot, we summed all aboveground biomass values and converted them to a per-unit area estimate (Mg ha^{-1}). Each site had 21 plots, except for one site, which had no marsh zone (14 plots). We first inventoried vegetation between November 2003 and February 2004, then used the same protocol to resample the plots between April and July 2016 (Taillie *et al* 2019).

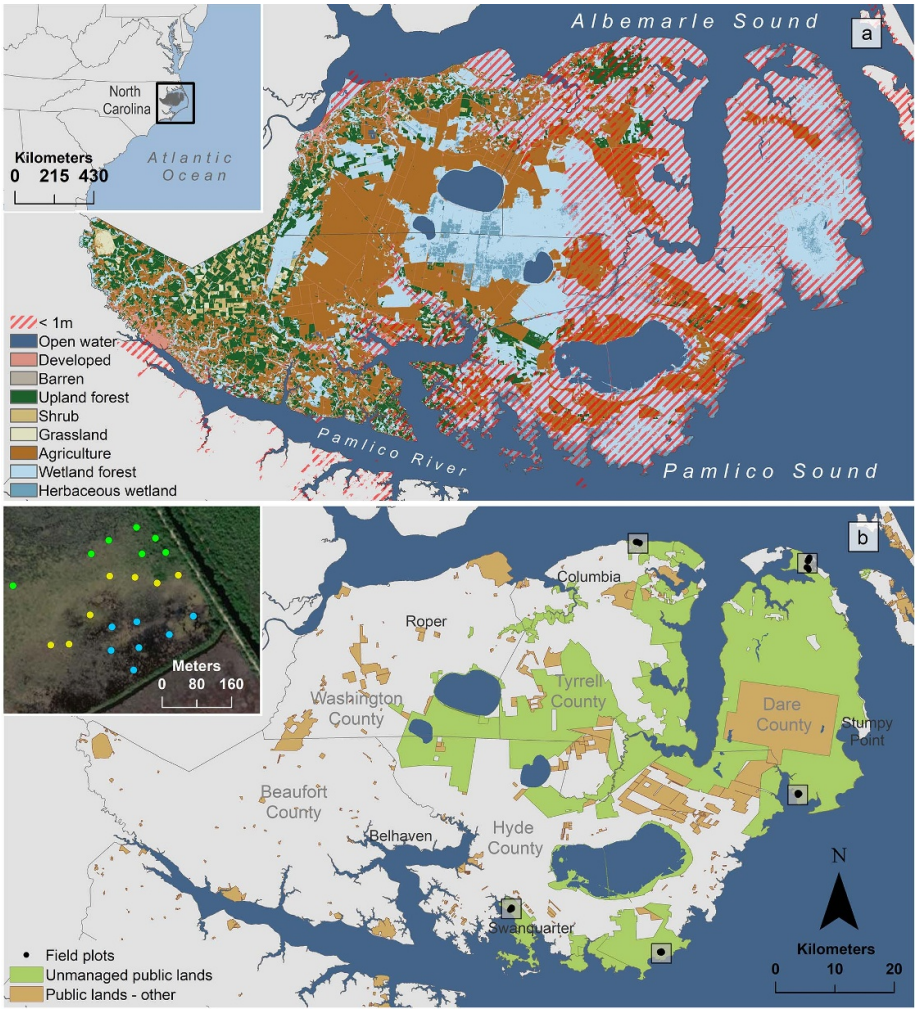

Figure 2. (a) The Albemarle-Pamlico Peninsula in eastern North Carolina, showing landcover (National Land Cover Database 2016 data) and areas less than 1 m in elevation. (b) Unmanaged and other public lands on the Albemarle-Pamlico Peninsula in eastern North Carolina. Ninety-eight field plots were established across five sites in the study area. At each site, plots were established across a vegetation gradient: forest, transition-ghost forest, and marsh (see example in inset map; forest plots are green, transition-ghost forest plots are yellow, and marsh plots are blue).

2.1. Mapping ghost forests

To identify ghost forest spread, we first mapped three vegetation classes of interest (forest, transition-ghost forest, and marsh) across the study area for two points in time: 2001 and 2014, using remotely sensed data from Landsat satellite imagery and Light Detection And Ranging (LiDAR) surveys.

We used all cloud-free images from Landsat 7 ETM + and Landsat 8 OLI from May-August (warm, wet period) and October-December (cool, dry period) for 2001 and 2014 (30-m resolution) to match the years of the available LiDAR data, preprocessing the data after Roy *et al* (2016) (US Geological Survey 2013, Google Earth Engine 2018). Spectral indices derived from Landsat included mean and maximum values for individual bands as well as derived vegetation indices including the Normalized Difference Vegetation Index (NDVI), Enhanced Vegetation Index (EVI), and tasseled cap indices (greenness, wetness, and brightness) (see table S1 for complete list of metrics).

We used LiDAR data, available from the North Carolina Floodplain Mapping Program's 2001 and 2014 statewide elevation mapping efforts (NOAA 2012, 2014), to generate landscape-scale vegetation height and density metrics across the study area. We created LiDAR vegetation metrics by subtracting the high-resolution digital elevation models (DEMs) derived for each year from the year's non-ground point clouds (the 2014 LiDAR dataset had a point density 18 times greater than the 2001 dataset, and so we analyzed each dataset independently; figure S1 available online at stacks.iop.org/ERL/15/104028/mmedia). We used 30-m resolution grids to match the spatial resolution of the Landsat data (see table S2 for complete list of metrics). We used permanent landmarks to align the Landsat- and LiDAR-based rasters. Vegetation heights

from the LiDAR data were binned into height strata by applying height thresholds associated with vegetation understory, midstory, and overstory (Hudak *et al* 2008, 2009, 2012, Smart *et al* 2012, Singh *et al* 2018).

We used the machine-learning algorithm Random Forest (RF, Breiman 2001; Evans and Cushman 2009; Evans *et al* 2011) as our classification method, using the '*randomForest*' package in R (Liaw 2018, RC Team 2018). We used the 2003 field measurements to train the 2001 model and the repeat field measurements from 2016 to train the 2014 model. For each model, we used the Model Improvement Ratio (MIR) to select the best predictor variables among the suite of candidate variables, after (Hudak *et al* 2012). We used a bootstrap approach to evaluate model performance. Using 1000 permutations of the final fitted RF model, we tested model significance, performed validation withholding 30% of the training data, and generated metrics of predictor variable importance (performed using '*rfUtillities*' and '*rfPermute*' in R; Archer 2018, Evans and Murphy 2018). Median and maximum vegetation height, EVI, tasseled cap indices (wetness), variance in vegetation heights, and NDVI were among the top predictor variables in both models (figure S2 and S3 for 2001 variable importance; S4 and S5 for 2014 variable importance). We performed a change analysis using these 2001 and 2014 vegetation class maps to quantify changes in forest extent and conversion from one vegetation class to another.

2.2. Measuring aboveground carbon

We identified the impacts of ghost forest proliferation on aboveground carbon by mapping total aboveground biomass (AGB) for two points in time: 2001 and 2014, using the metrics derived from LiDAR and Landsat satellite imagery as described in section 2.1.

We generated maps of aboveground biomass for the study area by regressing the remotely sensed vegetation metrics against the reference plots using the RF algorithm's regression model functionality. Maps of aboveground biomass values at 30-m resolution were generated from the RF models for the study area. We applied the methods described in section 2.1 for model building, training, and testing to select the best regression models for 2001 and 2014. Mean and median vegetation height, maximum vegetation height, variance in vegetation height, and NDVI were among the top performing predictors selected in the models (see figure S7 for variable importance).

Change in AGB for the study area was calculated as the difference between 2001 and 2014 AGB values and represented the net change over time, incorporating both gains from growth and losses from mortality or removal (Brienen *et al* 2015, Chen *et al* 2016). We reported change as an average value per unit area (Mg ha^{-1}) and a total (Tg) for the study area. We reported standard errors (S.E.) by propagating the error in the 2001 and 2014 AGB predictions (figure S8). We calculated aboveground carbon in 2001 and 2014 by applying vegetation-specific scaling factors (table S4; Byrd *et al* 2018; Martin *et al* 2018) to the AGB maps based on the vegetation classification maps. We calculated net aboveground carbon as the difference between 2001 and 2014 aboveground carbon values (TgC).

In 2008 and 2011, the study area was impacted by catastrophic wildfires (our field plots were unaffected). The 2008 Evans Road Fire covered approximately 165 km^2, affecting both unmanaged public lands and private lands. The 2011 Pains Bay Fire covered approximately 160 km^2 and affected both managed and unmanaged public lands. The Pains Bay Fire occurred close to the estuarine shoreline and the Evans Road Fire occurred in the central portion of the peninsula. We obtained spatial files of fire perimeters from the Monitoring Trends in Burn Severity (MTBS) dataset and estimated the impact of these fires on aboveground biomass and carbon (USDA Forest Service and US Geological Survey 2017).

To isolate changes in AGB and aboveground carbon associated with ghost forest spread from those resulting from other disturbance sources (e.g. wildfires and management activities on private lands), we provided multiple summaries of AGB change. We estimated AGB and carbon for (1) unmanaged public lands not impacted by fire; (2) unmanaged public lands including those impacted by fire; (3) unmanaged public lands and private lands not impacted by fire; (4) unmanaged public lands and private lands including those impacted by fire; and (5) only lands impacted by fires. To assign sections of the landscape to each of these categories, we overlaid our maps with the MTBS data layers and the North Carolina state department's managed areas dataset (NCNHP 2017).

2.3. Salinity and aboveground carbon dynamics

We used elevation and distance to shoreline as proxies for sea level rise vulnerability. Because artificial drainage networks also serve as conduits for saltwater intrusion if they are connected directly or indirectly to the estuarine shoreline, we used the National Hydrography Dataset to identify the estuarine shoreline and canals that were either directly or indirectly (connected via other canals) connected to the estuarine shoreline (US Geographical Survey 2018). We calculated the Euclidean distance from each part of the study area to the estuarine shoreline and connected canals.

We used salinity data from the Environmental Protection Agency's STORage and RETrieval (STORET) database for 40 water quality-monitoring sites in the sounds and canals adjacent to the study area (EPA 2017). We calculated mean salinity between 2001 and 2014 from 3500 + unique observations. As a proxy for soil salinity, we interpolated the average salinity values (in parts per thousand of NaCl) at each

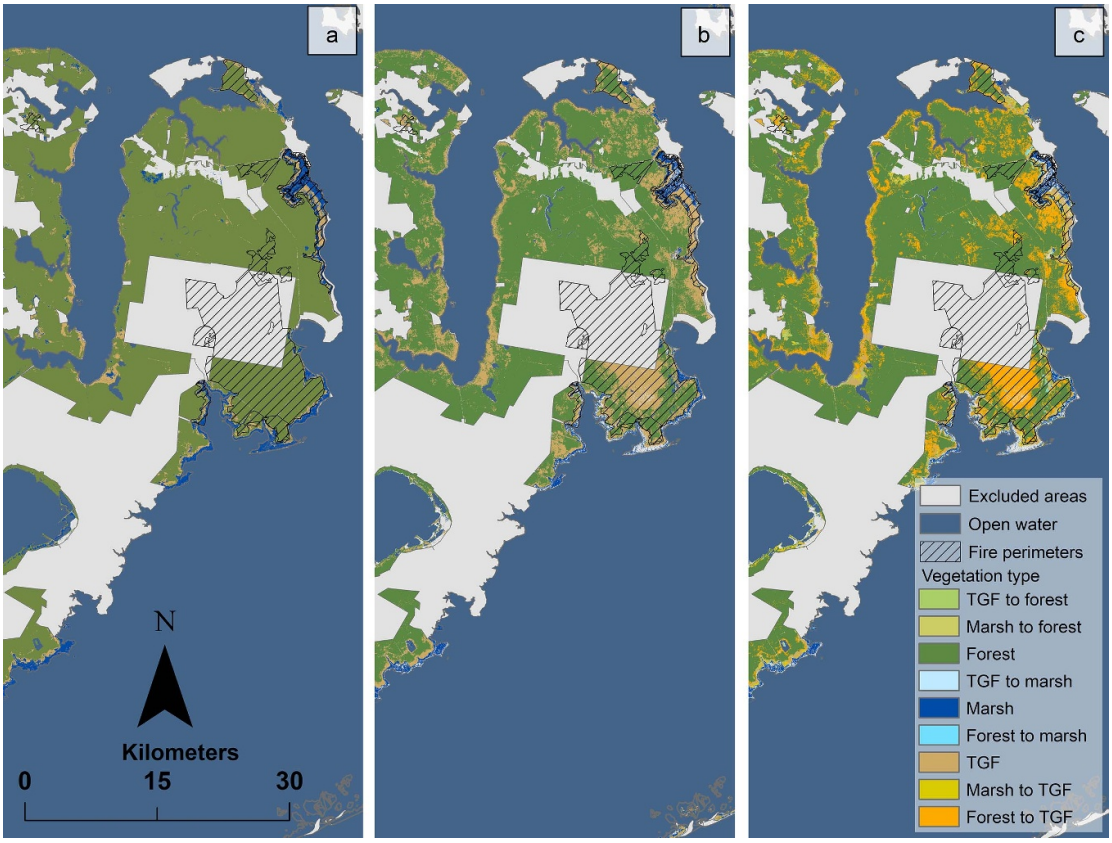

Figure 3. (a) Vegetation classification (forest, transition-ghost forest as TGF, and marsh) of the eastern portion of the Albemarle-Pamlico Peninsula, NC in 2001; (b) vegetation classification of the eastern portion in 2014; and (c) vegetation class change between 2001 and 2014.

of these locations across the study area using a spherical kriging method (Oliver and Webster 1990, Emadi and Baghernejad 2014).

We randomly selected a sample of 1000 locations on unmanaged public lands not impacted by fire in the study area for analysis (figure S12). We tested the relationships between our variables (distance to estuarine shoreline, distance to connected canals, salinity, elevation, and vegetation type in 2014) and aboveground biomass change (Mg ha^{-1}) using an Ordinary Least Squares (OLS) regression model. Global Moran's I tests on OLS residuals suggested significant spatial autocorrelation (p-value < 0.00001), so a spatial autoregressive error model (SEM) was used to fit the final model. We specified the spatial component of our error term using a row-normalized k-nearest neighborhood (k = 8) weight matrix. Regression analyses were performed using the '*spdep*' package in R (Bivand 2017).

3. Results

3.1. Mapping ghost forests

Classification error varied by vegetation class and year. In 2001, class error for forest was 6%, transition-ghost forest was 20%, and marsh was 18% (cv-kappa = 0.76, cv-out-of-bag error = 15%, cv-error variance = 0.0002). The model commonly misclassified forest as transition-ghost forest and transition-ghost forest as marsh (table S5). In 2014, class error for forest was 17%, transition-ghost was 40%, and marsh was 18% (cv-kappa = 0.60, cv-out-of-bag error = 26%, cv-error variance = 0.0003). The model commonly misclassified both marsh and forest as transition-ghost (table S6). Maximum vegetation height (for the 2001 model; figure S2, figure S3) and NDVI (for the 2014 model; figure S4, figure S5) were the highest performing predictors across all vegetation classes.

On unmanaged public lands not impacted by fire, there was a net loss of forest (152 km^2) between 2001 and 2014, with 167 km^2 of coastal forest converting to transition-ghost forest during this period; this change occurred on approximately 15% of the area. Conversion of transition-ghost forest to marsh comprised approximately 6 km^2 (0.5%). Between 2001 and 2014, 81% of the study area remained in the same forest vegetation type (figure 3(c), see table S7 for error estimates).

3.2. Measuring aboveground carbon

Total aboveground biomass models performed well, with the 2014 RF model performing slightly better ($R^2_{adj.}$ = 0.78, RMSE = 15.0 Mg ha^{-1}, % RMSE = 9.5) than the 2001 model ($R^2_{adj.}$ = 0.75, RMSE = 18.3 Mg ha^{-1}, % RMSE = 12.6) (figure S6).

Table 1. Measures of total area (km^2), mean aboveground biomass (AGB) change ($Mg\ ha^{-1}$), net aboveground biomass (Tg), and associated model standard errors (S.E.) for different landscape summary categories and for selected vegetation change classes for the Albemarle-Pamlico study area in eastern North Carolina, USA. In landscape category descriptions, '–' = 'excluding' and '+' = 'including'. Values for change classes are reported only for unmanaged public lands not including those impacted by fire.

	Total area	Mean AGB change (S.E.)	Net AGB (S.E.)
Landscape category			
Unmanaged public lands–fire	1138	10.7 (2.3)	1.21 (0.26)
Unmanaged public lands + fire	1381	6.0 (2.2)	0.83 (0.30)
Unmanaged public lands + private lands–fire	3320	14.4 (2.4)	4.67 (0.80)
Unmanaged public lands + private lands + fire	3716	11.0 (2.3)	3.96 (0.85)
Fire	396	−18.2 (1.3)	−0.71 (0.05)
Pains Bay fire	160	−16.7 (1.5)	−0.27 (0.02)
Evans Road fire	165	−24.2 (1.3)	−0.40 (0.02)
Change class			
No change forest[a]	828	17.8 (2.8)	1.49 (0.23)
Forest to transition-ghost forest	167	−16.2 (1.1)	−0.27 (0.02)
No change transition-ghost forest	39	−7.3 (0.8)	−0.03 (0.003)
Transition-ghost forest to marsh	6	−7.2 (0.4)	−0.004 (0.0002)

[a]Including unchanged forested private lands, net AGB is 4.90 ± 0.51 Tg (2.46 ± 0.25 TgC).

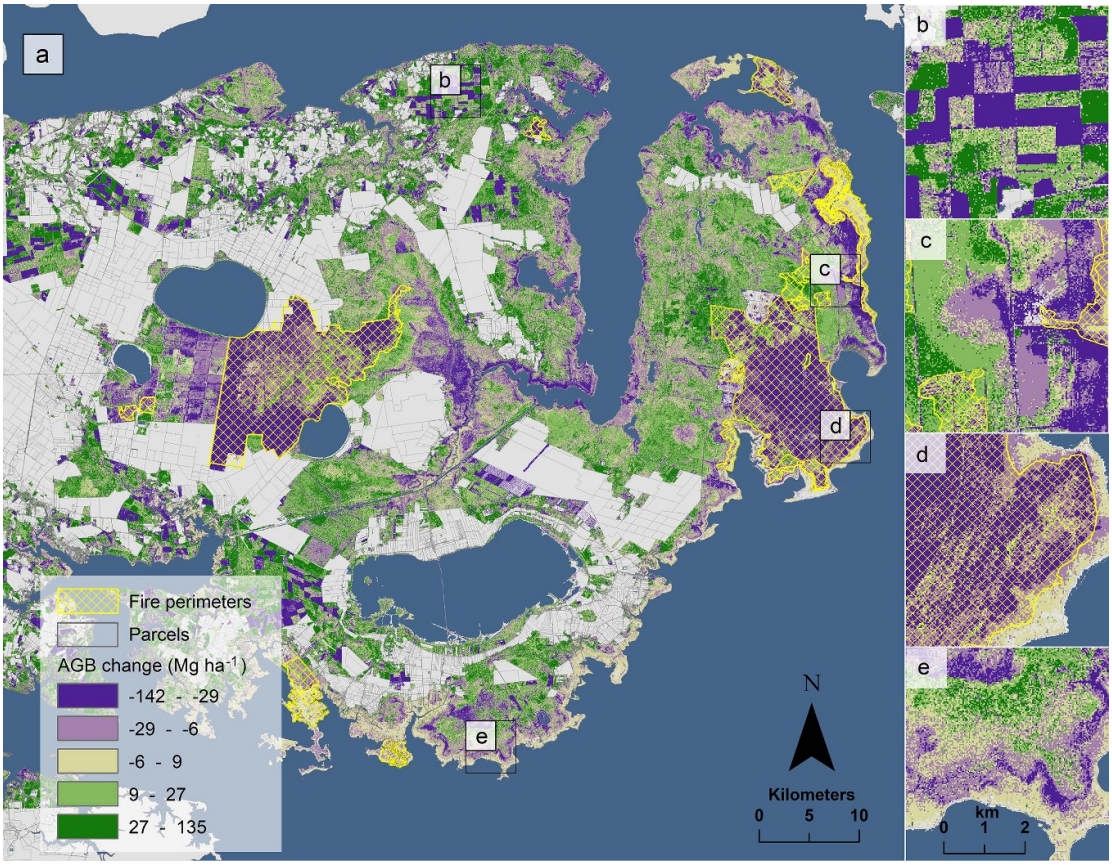

Figure 4. (a) Aboveground biomass change (AGB; measured in $Mg\ ha^{-1}$) on the Albemarle-Pamlico Peninsula in eastern North Carolina, USA. Grey areas are unmeasured areas (non-forested in 2001, e.g. developed lands or agricultural areas) and yellow crosshatched areas are fire perimeters provided by the Monitoring Trends in Burn Severity (MTBS) dataset. (b) An example of AGB change resulting from human land-use activities like planting and harvesting on pine plantations. (c) An example of AGB change along the shoreline in an unmanaged public portion of the landscape. (d) AGB change within the fire perimeter of the Pains Bay fire that occurred in 2011. (e) Characteristic pattern of forest dieback resulting from either an acute or gradual saltwater intrusion event (within Gull Rock Game Lands).

Mean and median vegetation height predictor variables contributed most to overall model performance, confirming the importance of vegetation structure to aboveground biomass estimation (figure S7). By vegetation type, predicted total aboveground biomass for the forested vegetation class (2001 $R^2_{adj.} = 0.96$, 2014 $R^2_{adj.} = 0.92$) outperformed the predicted AGB for the transition-ghost forest (2001 $R^2_{adj.} = 0.73$, 2014 $R^2_{adj.} = 0.76$, figure S9). Mapped aboveground biomass change between 2001 and 2014 accurately

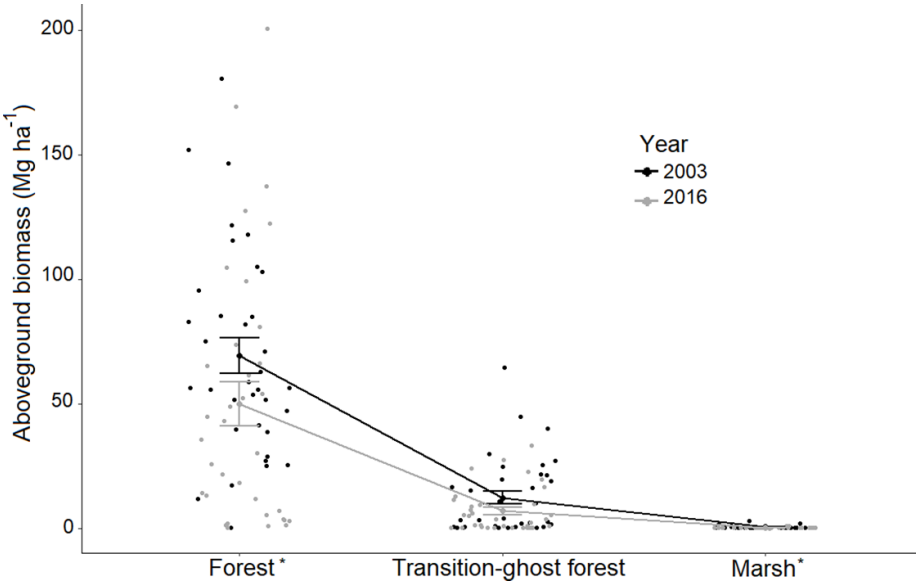

Figure 5. Mean field-measured aboveground biomass and associated standard errors (S.E.) by vegetation type (forest, transition-ghost forest, and marsh) and year (2003 = black, 2016 = light grey) for 98 plots distributed across 5 sites on the Albemarle-Pamlico Peninsula in eastern NC, USA. The * denotes a statistically significant difference between years using the Wilcoxon Signed Rank Test ($p < 0.05$). For more detailed marsh plots, see figure S11.

related to field-based estimates of aboveground biomass change between 2003 and 2016 ($R^2_{adj.} = 0.64$, RMSE = 13.4 Mg ha^{-1}, figure S10).

On unmanaged public lands not impacted by fire, change in AGB was positive (mean 10.7 ± 2.3 Mg ha^{-1}) with a net of 1.21 ± 0.26 Tg (6.2 Tg in 2001; 7.4 Tg in 2014). This equates to a 19% increase (0.53 ± 0.10 TgC) in aboveground carbon stores between 2001 and 2014 (table 1). Though carbon gains offset declines, biomass dynamics varied spatially, with losses occurring closer to the estuarine shoreline and gains more prevalent inland (figure 4(a)). We confirmed significant aboveground biomass declines (Wilcoxon Signed Rank test, $\alpha = 0.05$) in the field measurements during the study period (figure 5), with a total aboveground biomass loss overall of 8.8 ± 2.1 Mg ha^{-1} (p-value < 0.001); forest plots decreased in aboveground biomass by 28% (p-value < 0.05), and transition-ghost forest plots decreased by 39% (p-value = 0.2).

When the impacts of fire were included, AGB on unmanaged public lands only increased by 0.83 ± 0.30 Tg between 2001 and 2014, with mean 6.0 ± 2.2 Mg ha^{-1}.

Without fire, AGB on unmanaged public lands plus private lands increased by 4.67 ± 0.80 Tg (mean 14.4 ± 2.4 Mg ha^{-1}) between 2001 and 2014 but only increased by 3.96 ± 0.85 Tg (mean 11.0 ± 2.3 Mg ha^{-1}) when the impacts of fire were included.

Fire disturbances alone resulted in an overall AGB loss of 0.71 ± 0.05 Tg (−0.35 ± 0.05 TgC; figure 6) between 2001 and 2014. The Pains Bay fire (2011) resulted in an AGB loss of 0.27 ± 0.02 Tg (figure 4(d)) and the Evans Road fire (2008) resulted in an AGB loss of 0.40 ± 0.02 Tg (table 1).

By combining our vegetation class change maps from section 3.1 and AGB maps described above, we quantified between- and within-class changes in AGB (figure 7). Forested areas that remained forested between 2001 and 2014 experienced an overall net increase in AGB (17.8 ± 2.8 Mg ha^{-1}, table 1). This resulted in an aboveground carbon gain of 0.75 ± 0.12 TgC (2.46 ± 0.25 TgC when private lands are included). Conversion from forest to transition-ghost forest resulted in AGB loss (−16.2 ± 1.1 Mg ha^{-1}) and a 0.13 ± 0.01 TgC loss in aboveground carbon. Transition-ghost forest that remained transition-ghost forest experienced an overall net decline in aboveground biomass (−7.3 ± 0.8 Mg ha^{-1}).

3.3. Salinity and aboveground carbon dynamics

Using distance from the estuarine shoreline as a proxy for sea level rise vulnerability, we observed that areas closer to the shore (<1 km) had a net negative AGB change (−2.6 ± 0.8 Mg ha^{-1}), and areas farther from the shore (>1 km) had a net positive change (14.1 ± 0.9 Mg ha^{-1}) in AGB (Kruskal-Wallis test; p-value < 0.0001). Our salinity interpolation ranged from 0 ppt to a maximum of 18 ppt in our study area (figure 8(b)), very similar to soil water measurements collected at the field sites (Taillie *et al* 2019). Using a threshold of 2 ppt (Herbert *et al* 2015), areas with lower salinities (<2 ppt) gained more aboveground biomass between 2001 and 2014 (gain = 30.7 ± 0.8 Mg ha^{-1}) than areas with higher salinities (>2 ppt; gain = 12.8 ± 1.0 Mg ha^{-1}; Kruskal-Wallis test; p-value < 0.0001).

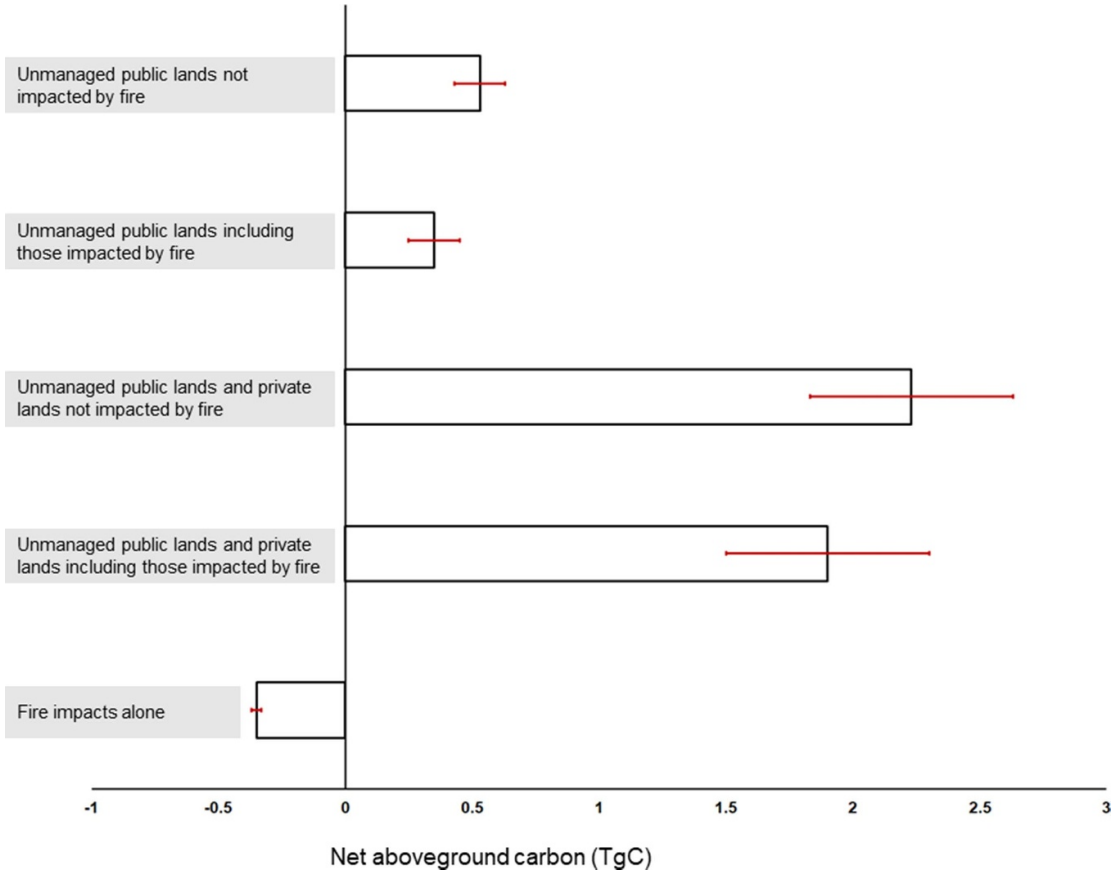

Figure 6. For the Albemarle-Pamlico Peninsula in eastern NC, USA, net aboveground carbon (TgC) and associated model standard errors summarized by: (1) unmanaged public lands not impacted by fire; (2) unmanaged public lands including those impacted by fire; (3) unmanaged public lands and private lands not impacted by fire; (4) unmanaged public lands and private lands including those impacted by fire; and (5) fire impacts alone.

Results from our spatial error model indicated that salinity was negatively related to aboveground biomass; as salinity increases AGB decreases (p-value < 0.01). Connected canal distance was also negatively related to aboveground biomass (p-value < 0.01). The effect of elevation on aboveground biomass differed based on the characteristic vegetation type present in 2014; elevation was positively related to aboveground biomass in the marsh and transition-ghost forest vegetation types but negatively related to aboveground biomass in areas classified as forest (table 2).

4. Discussion

Our results highlight that, although aboveground carbon declines are apparent nearshore, land management activities and forest growth offset these declines. As the landward extent of sea level rise impact increases, this study highlights potential opportunities for targeted human interventions to preserve the region's carbon sink. Studies in highly dynamic coastal systems at fine scales across broad spatial extents are rare, posing challenges for monitoring and forecasting coastal ecosystem change. However, with increasing availability of data from aerial- and satellite-based LiDAR platforms, our methods can be applied in other low-lying coastal plains to develop landscape-scale measurements of historical impacts from sea level rise and identify areas most vulnerable to future impacts. Investigations at these large scales are requisite for allocating resources for monitoring, targeting interventions, and adapting to a changing environment.

Coastal vegetation transitions are driven by complex interactions between gradual climate changes and episodic disturbance events. Impacts from gradual inundation alone occur at long (e.g. centuries) temporal scales (Schieder *et al* 2018, Schieder and Kirwan 2019). At much shorter time scales (such as the one evaluated in this study), it is more likely for episodic disturbances to drive vegetation changes (Poulter *et al* 2009). However, the frequency, extent, and severity of disturbances can be exacerbated or mediated by climate change (Bender *et al* 2010). Droughts, as an example, are expected to increase in duration and severity as the climate changes, increasing saltwater exposure in freshwater ecosystems (via landward movement of the freshwater-saltwater interface) (Ardón *et al* 2016). These complex interactions (Herbert *et al* 2015), in addition to land-use impediments like upslope agricultural fields

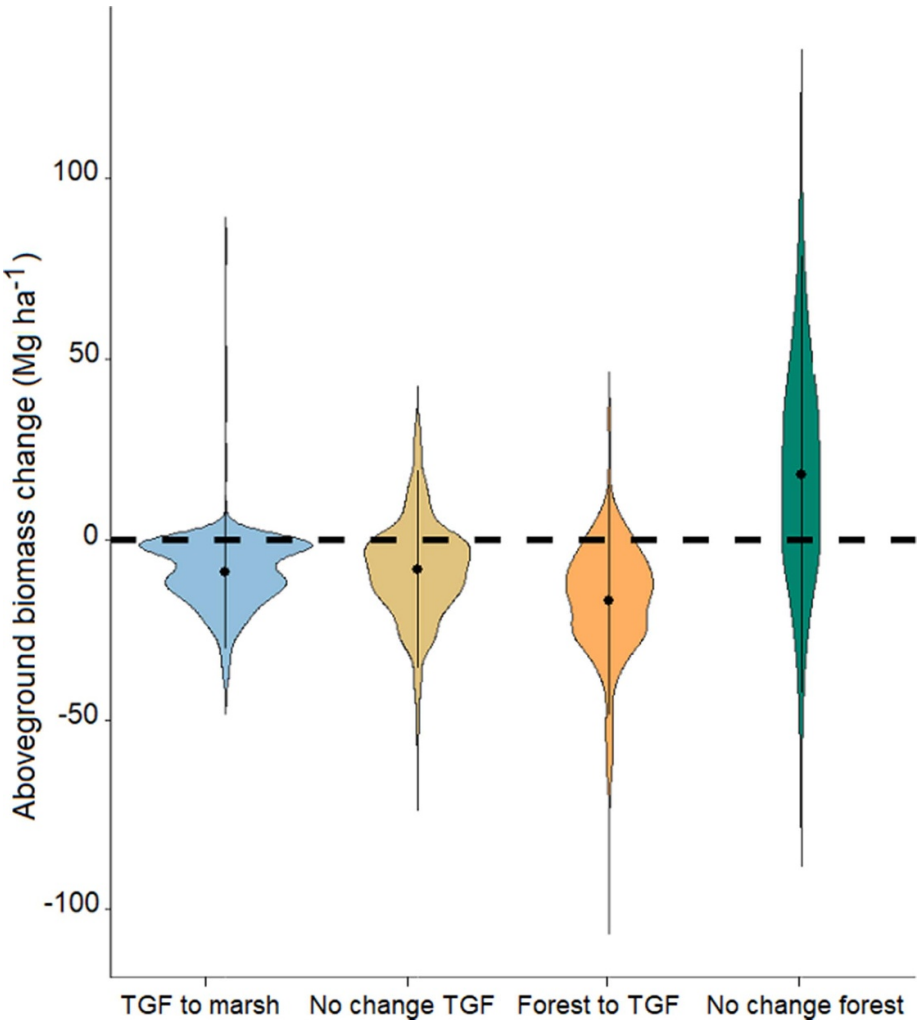

Figure 7. Violin plots of aboveground biomass change (sampled at 500-m intervals across unmanaged public lands not impacted by fire on the Albemarle-Pamlico Peninsula in eastern NC, USA) summarized by vegetation type change (transition-ghost forest abbreviated as TGF).

or urban development (Enwright *et al* 2016, Borchert *et al* 2018), will ultimately determine the spatiotemporal patterns of forest retreat in coastal systems.

Between 2001 and 2014, we measured conversion from forest to a short (<5 m) shrub-dominated transition phase on 15% of unmanaged public lands in our study area. Analyzing temporal shifts in species composition using the same field plots as this study, Taillie *et al* (2019) confirmed low tree regeneration between 2003 and 2016. Corroborating previous field studies (Raabe and Stumpf 2016, Langston *et al* 2017), their results indicated a general shift in vegetation towards more salt-tolerant shrubs and herbaceous vegetation over the course of the study (Taillie *et al* 2019). From our regression models, we identified differential impacts of elevation on aboveground biomass across vegetation types. The counterintuitive result for forests (a negative relationship between forest aboveground biomass and elevation) may reflect the inclusion of unknown human land-use management on public lands affecting forest structure and species composition and/or drainage patterns. It may also reflect the overall decrease in aboveground biomass variability as elevation increases or the transition into a forest class with lower aboveground biomass. Both our spatial predictions and regression models indicated that aboveground biomass and carbon declines were more likely near the estuarine shoreline and in areas with higher salinities. This supports other studies that have demonstrated the importance of salinization as a stronger driver of coastal forest change than elevation and inundation alone (Krauss *et al* 2007, Craft 2012, Taillie *et al* 2019). Shorelines, creeks, and artificial drainages can serve as conduits for saltwater to move inland, causing forest dieback in areas proximal to these landscape features (Herbert *et al* 2015, Krauss *et al* 2018, Ury *et al* 2020).

Human activities on private lands at higher elevations in the study area resulted in heterogeneous patterns of both aboveground carbon gains and declines. However, their net contribution to aboveground carbon storage was positive. Carbon dynamics on private lands in the study area result from individual land-use decisions, including planting and harvesting

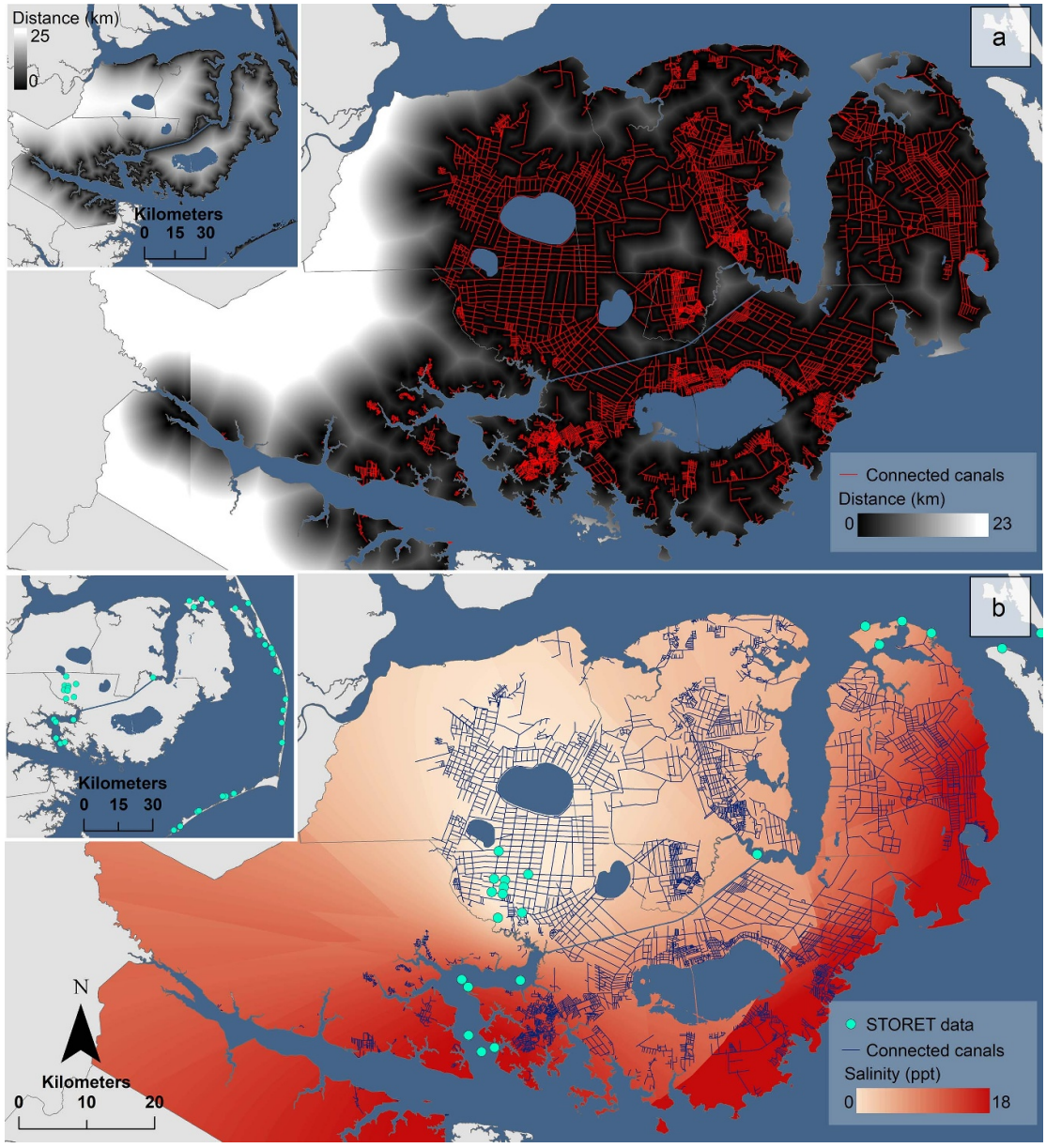

Figure 8. (a) Euclidean distance to connected canals; inset = Euclidean distance to estuarine shoreline only. (b) Salinity interpolation, measured in parts per thousand (ppt), using the 40 water quality monitoring stations along the Albemarle and Pamlico Sounds in eastern North Carolina; inset = all points used in salinity interpolation from the Environmental Protection Agency's STORET database. High salinities occur along the estuarine shoreline in the east and gradually decrease westward, with increasing distance from the shoreline. High salinities also occur in the southern part of the peninsula, resulting from proximity to the more saline Pamlico Sound, with decreasing salinities northward closer to the near-fresh Albemarle Sound.

of timber and hydrologic modification via artificial drainages and canals. Though meant to move water off lands, the extensive drainage networks in our study area are also susceptible to saltwater intrusion from gradual inundation and hurricanes (Manda *et al* 2014; Bhattachan *et al* 2018). The efficacy of the networks is highly dependent upon landowner management (Poulter *et al* 2008). Our spatial regression model showed that, on unmanaged public lands, aboveground biomass declines were more prevalent farther from drainage networks. This may seem counterintuitive, but it is possible that active management of drainage networks on public lands has lessened the extent of saltwater intrusion. On private lands, the relationship between biomass and canals might differ because landowner objectives and resources may not match those of public land managers. To prevent net carbon loss associated with climate change and sea level rise, opportunities exist on private lands to increase carbon through management activities like reforestation, lengthened harvest cycles, and restricting harvests. These land management decisions also have numerous co-benefits including increases in water availability and biodiversity (Law *et al* 2018). Human land management decisions and interventions on the Albemarle-Pamlico Peninsula will largely determine the continued ability of the region to serve as a carbon sink.

Table 2. Parameter estimates and standard errors ('S.E.') for the ordinary least squares (OLS) regression model and the spatial error model (SEM) to test the relationship between aboveground biomass change (Mg ha^{-1}) and five potential drivers at 1000 random locations on the Albemarle-Pamlico Peninsula in NC, USA. Akaike information criterion (AIC), pseudo-R squared, and Moran's I residuals are also provided.

	OLS estimate (S.E.)	SEM estimate (S.E.)
(Intercept)	38.0 (3.1)***	30.0 (4.6)***
Salinity	−1.8 (0.4)***	−1.7 (0.7)**
Distance to estuarine shoreline	1.5 (0.5)**	1.9 (0.9)*
Distance to connected canals	−3.9 (1.0)***	−3.2 (1.4)**
Transition-ghost forest	−14.4 (23.2)	−20.8 (21.8)
Marsh	−46.2 (5.8)***	−41.2 (5.5)***
Elevation	−27.0 (4.7)***	−24.7 (5.1)***
Salinity: distance to estuarine shoreline	0.1 (0.1)	0.2 (0.2)
Transition-ghost forest: elevation	13.3 (64.3)	27.1 (59.6)
Marsh: elevation	34.4 (10.0)***	31.0 (9.5)***
AIC	9313.7	9245.1
Moran's I residual	0.1***	0.0
(Pseudo- R squared)	0.27	0.32

Significance codes: 0 '***' 0.001 '**' 0.01 '*' 0.05 '.' 0.1 ' ' 1

Fire disturbance may also facilitate the progression from forest to marsh on salt-affected lands. Frequent, low-intensity fires have historically maintained vegetation structure in these coastal ecosystems (Frost 1995, Poulter *et al* 2009). Post-fire, we would expect to see regeneration as part of natural forest succession. Comparing two catastrophic wildfires that occurred during our study period—one in 2008 (Evans Road fire) in the study area center and another in 2011 (Pains Bay fire) near the estuarine shoreline—we find less regeneration than expected (Frost 1995), as indicated by the aboveground carbon estimates, within the fire perimeters near the shoreline. Fire disturbance and saltwater intrusion may have an interactive effect that inhibits woody species growth and promotes marsh migration landward. Seedlings and saplings of freshwater woody species need sufficient time to establish post-fire, but if saltwater exposure occurs before these saplings have established, post-fire regeneration will be reduced (Poulter *et al* 2008). Although fires have historically played a significant role in maintaining vegetation structure and composition in this region, this role may be changing along with the changing climate.

Saltwater intrusion from sea level rise is often considered an 'invisible' threat because shifts in soil chemistry are difficult to measure at large spatial scales and are not generally perceived by the public (Tully *et al* 2019). However, ghost forests provide clear markers of sea level rise's leading edge. There is still a great deal of uncertainty about system-level impacts of salinization on net carbon (Henman and Poulter 2008), with recent research highlighting divergent biogeochemical responses of soils to saltwater intrusion (Ardón *et al* 2013, Herbert *et al* 2015, Helton *et al* 2019). Future work that quantifies the landscape-scale impacts of saltwater intrusion on different carbon pools, would complement our estimates of aboveground carbon. As rates of sea level rise accelerate and the landward extent of impact increases, a better understanding of the spatiotemporal patterns of forest retreat and aboveground carbon in coastal systems is essential for developing effective management and adaptation plans. Our research provides a critical baseline, from which policy makers, landowners, and managers can draw, to better anticipate the interventions and adaptation activities necessary in both the near- and far-term.

Acknowledgments

We are grateful to Dr Megan Skrip from the Center for Geospatial Analytics for edits and comments that greatly improved the quality of this manuscript. We thank Dr Vaclav Petras of NC State University, who provided technical insights and troubleshooting during the LiDAR data processing phase in GRASS GIS. Additionally, Douglas Newcomb of the U.S. Fish and Wildlife Service, provided valuable comments on methods and analyses. Finally, we thank the three anonymous reviewers whose comments greatly improved this manuscript.

Funding

This research was funded by a joint fellowship through NOAA's North Carolina Sea Grant Program and NASA's North Carolina Space Grant Program (NOAA award # NA14OAR4170073, NASA award # NNX15AH81H). Funding from a College of Natural Resources Innovation Grant at NC State University was also used to support this research.

Conflicts of interest

The authors declare no conflict of interest.

ORCID iDs

Paul J Taillie https://orcid.org/0000-0001-7172-3589
Jelena Vukomanovic https://orcid.org/0000-0001-6477-6551
Kunwar K Singh https://orcid.org/0000-0002-9788-1822
Jennifer J Swenson https://orcid.org/0000-0002-2069-667X
Jordan W Smith https://orcid.org/0000-0001-7036-4887

References

Archer E 2018 *rfPermute*. R package version 2. 1.81 (available at: https://cran.r-project.org/web/packages/rfPermute/index.html) (Accessed January 2017)
Ardón M, Helton A M and Bernhardt E S 2016 Drought and saltwater incursion synergistically reduce dissolved organic carbon export from coastal freshwater wetlands *Biogeochemistry* **127** 411–26
Ardón M, Morse J L, Colman B P and Bernhardt E S 2013 Drought-induced saltwater incursion leads to increased wetland nitrogen export *Glob. Chang. Biol.* **19** 2976–85
Bender M A, Knutson T R, Tuleya R E, Sirutis J J, Vecchi G A, Garner S T and Held I M 2010 Modeled impact of anthropogenic warming on the frequency of intense Atlantic hurricanes *Science* **327** 454–8
Bhattachan A, Emanuel R E, Ardon M, Bernhardt E S, Anderson S M, Stillwagon M G, Ury E A, Bendor T K and Wright J P 2018 Evaluating the effects of land-use change and future climate change on vulnerability of coastal landscapes to saltwater intrusion *Elem. Sci. Anth.* **6** 62
Barbier E B, Hacker S D, Kennedy C, Koch E W, Stier A C and Silliman B R 2011 The value of estuarine and coastal ecosystem services *Ecol. Monographs* **81** 169–93
Bivand R 2017 *spdep*. R package version 2. 1.81 (available at: https://cran.r-project.org/web/packages/spdep/index.html) (Accessed January 2017)
Borchert S M, Osland M J, Enwright N M and Griffith K T 2018 Coastal wetland adaptation to sea level rise: quantifying potential for landward migration and coastal squeeze *J. Appl. Ecol.* **55** 2876–87
Breiman L 2001 Random forests *Mach. Learn.* **45** 5–32
Brienen R J *et al* 2015 Long-term decline of the Amazon carbon sink *Nature* **519** 344–8
Brinson M M, Christian R R and Blum L K 1995 Multiple states in the sea-level induced transition from terrestrial forest to estuary *Estuaries* **18** 648–59
Byrd K B, Ballanti L, Thomas N, Nguyen D, Holmquist J R, Simard M and Windham-Myers L 2018 A remote sensing-based model of tidal marsh aboveground carbon stocks for the conterminous United States *ISPRS J. Photogramm. Remote Sens.* **139** 255–71
Castillo J M, Leira-Doce P, Rubio-Casal A E and Figueroa E 2008 Spatial and temporal variations in aboveground and belowground biomass of Spartina maritima (small cordgrass) in created and natural marshes *Estuar. Coast Shelf Sci.* **78** 819–26
Chen H Y, Luo Y, Reich P B, Searle E B and Biswas S R 2016 Climate change-associated trends in net biomass change are age dependent in western boreal forests of Canada *Ecol. Lett.* **19** 1150–8
Church J A *et al* 2013 Sea level change *Climate Change 2013: The Physical Science Basis. Contribution of Working Group I to the Fifth Assessment Report of the Intergovernmental Panel on Climate Change* ed T F Stocker *et al* (Cambridge: Cambridge University Press)
Church J A and White N J 2011 Sea-level rise from the late 19th to the early 21st century *Surv. Geophys.* **32** 585–602
Conner W H, Doyle T W and Krauss K R 2007 *Ecology of Tidal Forested Wetlands of the Southeastern United States* (Berlin: Springer)
Craft C B 2012 Tidal freshwater forest accretion does not keep pace with sea level rise *Glob. Chang. Biol.* **18** 3615–23
Dangendorf S, Marcos M, Wöppelmann G, Conrad C P, Frederikse T and Riva R 2017 Reassessment of 20th century global mean sea level rise *Proc. Natl Acad. Sci.* **114** 5946–51
DeSantis L R, Bhotika S, Williams K and Putz F E 2007 Sea-level rise and drought interactions accelerate forest decline on the Gulf Coast of Florida, USA *Glob. Chang. Biol.* **13** 2349–60
Duarte C M and Prairie Y T 2005 Prevalence of heterotrophy and atmospheric CO_2 emissions from aquatic ecosystems *Ecosystems* **8** 862–70
Emadi M and Baghernejad M 2014 Comparison of spatial interpolation techniques for mapping soil pH and salinity in agricultural coastal areas, northern Iran *Arch. Agron. Soil Sci.* **60** 1315–27
Environmental Protection Agency 2017 STORage and RETrieval Warehouse/Water Quality Exchange (available at: www3.epa.gov/storet/bck/dbtop.html) (Accessed January 2017)
Enwright N M, Griffith K T and Osland M J 2016 Barriers to and opportunities for landward migration of coastal wetlands with sea-level rise *Front Ecol. Environ.* **14** 307–16
Erwin K L 2009 Wetlands and global climate change: the role of wetland restoration in a changing world *Wetland Ecol. Manag.* **17** 71
Evans J S and Cushman S A 2009 Gradient modeling of conifer species using random forests *Landsc. Ecol.* **24** 673–83
Evans J S and Murphy M A 2018 *rfUtilities*. R package version 2.1.6 (available at: https://cran.r-project.org/web/packages/rfUtilities/index.html) (Accessed January 2017)
Evans J S, Murphy M A, Holden Z A and Cushman S A 2011 Modeling species distribution and change using random forest *Predictive Species and Habitat Modeling in Landscape Ecology* ed C Drew, Y Wiersman and F Huettmann (Berlin: Springer) pp 139–59
Field C R, Gjerdrum C and Elphick C S 2016 Forest resistance to sea-level rise prevents landward migration of tidal marsh *Biol. Conserv.* **201** 363–9
Frost C C 1995 Presettlement fire regimes in southeastern marshes, peatlands, and swamps *Proc. 19th Tall Timbers Fire Ecology Conference: Fire in Wetlands: A Management Perspective* (Tallahassee, FL: Tall Timbers Research Inc.)
Gibbon A, Silman M R, Malhi Y, Fisher J B, Meir P, Zimmermann M, Dargie G C, Farfan W R and Garcia K C 2010 Ecosystem carbon storage across the grassland–forest transition in the high Andes of Manu National Park, Peru *Ecosystems* **13** 1097–111
Google Earth Engine 2018 A planetary-scale platform for Earth science data & analysis (available at: https://earthengine.google.com/) (Accessed December 2017)
Hackney C T and Yelverton G F 1990 Effects of human activities and sea level rise on wetland ecosystems in the Cape Fear River Estuary, North Carolina, USA *Wetland Ecology and Management: Case Studies* (Berlin: Springer) pp 55–61
Hamilton S E and Casey D 2016 Creation of a high spatio-temporal resolution global database of continuous mangrove forest cover for the 21st century (CGMFC-21) *Glob. Ecol. Biogeogr.* **25** 729–38
He Q and Silliman B R 2019 Climate change, human impacts, and coastal ecosystems in the Anthropocene *Curr. Biol.* **29** R1021–35
Helton A M, Ardón M and Bernhardt E S 2019 Hydrologic context alters greenhouse gas feedbacks of coastal wetland salinization *Ecosystems* **22** 1108–25

Henman J and Poulter B 2008 Inundation of freshwater peatlands by sea level rise: uncertainty and potential carbon cycle feedbacks *J. Geophys. Res.* **113** G01011

Herbert E R, Boon P, Burgin A J, Neubauer S C, Franklin R B, Ardón M, Hopfensperger K N, Lamers L P and Gell P 2015 A global perspective on wetland salinization: ecological consequences of a growing threat to freshwater wetlands *Ecosphere* **6** 1–43

Hudak A T, Crookston N L, Evans J S, Hall D E and Falkowski M J 2008 Nearest neighbor imputation of species-level, plot-scale forest structure attributes from LiDAR data *Remote Sens. Environ.* **112** 2232–45

Hudak A T, Evans J S and Stuart Smith A M 2009 LiDAR utility for natural resource managers *Remote Sens.* **1** 934–51

Hudak A T, Strand E K, Vierling L A, Byrne J C, Eitel J U, Martinuzzi S and Falkowski M J 2012 Quantifying aboveground forest carbon pools and fluxes from repeat LiDAR surveys *Remote Sens. Environ.* **123** 25–40

Jenkins J C, Chojnacky D C, Heath L S and Birdsey R A 2003 National-scale biomass estimators for United States tree species *Forest Sci.* **49** 12–35

Karegar M A, Dixon T H and Engelhart S E 2016 Subsidence along the Atlantic Coast of North America: insights from GPS and late Holocene relative sea level data *Geophys Res. Lett.* **43** 3126–33

Karegar M A, Dixon T H, Malservisi R, Kusche J and Engelhart S E 2017 Nuisance flooding and relative sea-level rise: the importance of present-day land motion *Sci. Rep.* **7** 1–9

Kirschbaum M U, Saggar S, Tate K R, Giltrap D L, Ausseil A G E, Greenhalgh S and Whitehead D 2012 Comprehensive evaluation of the climate-change implications of shifting land use between forest and grassland: New Zealand as a case study *Agric. Ecosyst. Environ.* **150** 123–38

Kirwan M L, Kirwan J L and Copenheaver C A 2007 Dynamics of an estuarine forest and its response to rising sea level *J. Coastal Res.* **23** 457–63

Kirwan M L and Gedan K B 2019 Sea-level driven land conversion and the formation of ghost forests *Nat. Clim. Chang.* **9** 450–7

Kirwan M L and Megonigal J P 2013 Tidal wetland stability in the face of human impacts and sea-level rise *Nature* **504** 53–60

Krauss K W, Chambers J L and Creech D 2007 Selection for salt tolerance in tidal freshwater swamp species: advances using baldcypress as a model for restoration *Ecology of Tidal Freshwater Forested Wetlands of the Southeastern United States* ed W H Conner, T W Doyle and K W Krauss (Berlin: Springer) pp 385–410

Krauss K W *et al* 2017 Created mangrove wetlands store belowground carbon and surface elevation change enables them to adjust to sea-level rise *Sci. Rep.* **7** 1–11

Krauss K W, Doyle T W, Conner W H and Duberstein J A 2009 Research insight from tidal freshwater forested wetlands *Wetland Sci. Practice* **26** 18–21

Krauss K W *et al* 2018 The role of the upper tidal estuary in wetland blue carbon storage and flux *Glob. Biogeochem. Cycles* **32** 817–39

Lagomasino D, Fatoyinbo T, Lee S, Feliciano E, Trettin C, Shapiro A and Mangora M M 2019 Measuring mangrove carbon loss and gain in deltas *Environ. Res. Lett.* **14** 025002

Langston A K, Kaplan D A and Putz F E 2017 A casualty of climate change? Loss of freshwater forest islands on Florida's Gulf Coast *Glob. Chang. Biol.* **23** 5383–97

Law B E, Hudiburg T W, Berner L T, Kent J J, Buotte P C and Harmon M E 2018 Land use strategies to mitigate climate change in carbon dense temperate forests *Proc. Natl Acad. Sci.* **115** 3663–8

Liaw A 2018 *randomforest*. R package version 2. 1.81 (available at: https://cran.r-project.org/web/packages/randomForest/index.html) (Accessed December 2016)

Manda A K, Giuliano A S and Allen T R 2014 Influence of artificial channels on the source and extent of saline water intrusion in the wind tide dominated wetlands of the southern Albemarle estuarine system (USA) *Environ. Earth Sci.* **71** 4409–19

Martin A R, Doraisami M and Thomas S C 2018 Global patterns in wood carbon concentration across the world's trees and forests *Nat. Geosci.* **11** 915–20

McLeod E, Chmura G L, Bouillon S, Salm R, Björk M, Duarte C M, Lovelock C E, Schlesinger W H and Silliman B R 2011 A blueprint for blue carbon: toward an improved understanding of the role of vegetated coastal habitats in sequestering CO_2 *Front Ecol. Environ.* **9** 552–60

McNulty S *et al* 2015 *Southeast Regional Climate Hub Assessment of Climate Change Vulnerability and Adaptation and Mitigation Strategies* (Washington, DC: United States Department of Agriculture)

Millennium Ecosystem Assessment 2005 *Ecosystems and Human Well-being* (Washington, DC: World Resources Institute)

Moorhead K K and Brinson M M 1995 Response of wetlands to rising sea level in the lower coastal plain of North Carolina *Ecol. Appl.* **5** 261–71

Moorman C E, Russell K R, Sabin G R and Guynn Jr D C 1999 Snag dynamics and cavity occurrence in the South Carolina Piedmont *For. Ecol. Manage.* **118** 37–48

National Oceanic and Atmospheric Administration 2014 2014 NCFMP Lidar: Phase (available at: https://coast.noaa.gov/digitalcoast/) (Accessed 1 December 2016)

National Oceanic and Atmospheric Administration 2012 2001 NCFMP Lidar: Phase (available at: https://coast.noaa.gov/digitalcoast/) (Accessed 1 December 2016)

Noe G B, Hupp C R, Bernhardt C E and Krauss K W 2016 Contemporary deposition and long-term accumulation of sediment and nutrients by tidal freshwater forested wetlands impacted by sea level rise *Estuar. Coast.* **39** 1006–19

North Carolina Natural Heritage Program 2017 Geographic Information System (GIS) data. NCDNCR, Raleigh, NC (available at: www.ncnhp.org (Accessed January 2017)

Oliver M A and Webster R 1990 Kriging: a method of interpolation for geographical information systems *Int. J. Geogr. Inform. Syst.* **4** 313–32

Pendleton L *et al* 2012 Estimating global "blue carbon" emissions from conversion and degradation of vegetated coastal ecosystems *PLoS ONE* **7** e43542

Poulter B 2005 Interactions between landscape disturbance and gradual environmental change: plant community migration in response to fire and sea-level rise *PhD Dissertation* Duke University, Durham, NC

Poulter B, Christensen N L Jr and Halpin P N 2006 Carbon emissions from a temperate peat fire and its relevance to interannual variability of trace atmospheric greenhouse gases *J. Geophys. Res.: Atmos.* **111** D06301

Poulter B, Goodall J L and Halpin P N 2008 Applications of network analysis for adaptive management of artificial drainage systems in landscapes vulnerable to sea level rise *J. Hydrol.* **357** 207–17

Poulter B, Qian S S and Christensen N L 2009 Determinants of coastal treeline and the role of abiotic and biotic interactions *Plant Ecol.* **202** 55–66

Raabe E A and Stumpf R P 2016 Expansion of tidal marsh in response to sea-level rise: gulf Coast of Florida, USA *Estuar. Coast.* **39** 145–57

RC Team 2018 R Core Team. R: a language and environment for statistical computing (available at: https://cran.r-project.org/) (Accessed December 2016)

Riegel J B, Bernhardt E and Swenson J 2013 Estimating above-ground carbon biomass in a newly restored coastal plain wetland using remote sensing *PLoS ONE* **8** e68251

Roy D P, Kovalskyy V, Zhang H K, Vermote E F, Yan L, Kumar S S and Egorov A 2016 Characterization of Landsat-7 to Landsat-8 reflective wavelength and normalized difference vegetation index continuity *Rem. Sens. Environ.* **185** 57–70

Schieder N W and Kirwan M L 2019 Sea-level driven acceleration in coastal forest retreat *Geology* **47** 1151–5

Schieder N W, Walters D C and Kirwan M L 2018 Massive upland to wetland conversion compensated for historical marsh loss in Chesapeake Bay, USA *Estuar. Coast.* **41** 940–51

Simard M, Fatoyinbo L, Smetanka C, Rivera-Monroy V H, Castañeda-Moya E, Thomas N and Van der Stocken T 2019 Mangrove canopy height globally related to precipitation, temperature and cyclone frequency *Nat. Geosci.* **12** 40–5

Singh K K, Smart L S and Chen G 2018 LiDAR and spectral data integration for coastal wetland assessment *High Spatial Resolution Remote Sensing: Data, Analysis, and Applications* (Boca Raton, FL: CRC Press) pp 71–88

Smart L S, Swenson J J, Christensen N L and Sexton J O 2012 Three-dimensional characterization of pine forest type and red-cockaded woodpecker habitat by small-footprint, discrete-return lidar *For. Ecol. Manage.* **281** 100–10

Smith W B and Brand G J 1983 Allometric biomass equations for 98 species of herbs, shrubs, and small trees *Research Note NC-299. St. Paul, MN: US Dept. of Agriculture, Forest Service, North Central Forest Experiment Station*

Taillie P J, Moorman C E, Poulter B, Ardon M and Emanuel R E 2019 Decadal-scale vegetation change driven by salinity at leading edge of rising sea level *Ecosystems* **22** 1918–30

Thomas N, Lucas R, Bunting P, Hardy A, Rosenqvist A and Simard M 2017 Distribution and drivers of global mangrove forest change, 1996–2010 *PLoS ONE* **12** e0179302

Trilla G G, Kandus P, Negrin V, Vicari R and Marcovecchio J 2009 Tiller dynamic and production on a SW Atlantic Spartina alterniflora marsh *Estuar. Coast Shelf Sci.* **85** 126–33

Tully K *et al* 2019 The invisible flood: the chemistry, ecology, and social implications of coastal saltwater intrusion *BioScience* **69** 368–78

Ury E A, Anderson S M, Peet R K, Bernhardt E S and Wright J P 2020 Succession, regression and loss: does evidence of saltwater exposure explain recent changes in the tree communities of North Carolina's Coastal Plain? *Ann. Bot.* **125** 255–64

US Geographical Survey 2018 GloVis Data Warehouse (available at: http://glovis.usgs.gov) (Accessed December 2016)

US Geological Survey 2013 National Hydrography Geodatabase: The National Map Viewer (available at: http://nhd.usgs.gov/data.html) (Accessed May 2016)

USDA Forest Service and US Geological Survey 2017 MTBS Data Access: Fire Level Geospatial Data (available at: http://mtbs.gov/direct-download) (Accessed 1 May 2017)

White E and Kaplan D 2017 Restore or retreat? Saltwater intrusion and water management in coastal wetlands *Ecosyst. Health Sustain.* **3** e01258

Williams K, Ewel K C, Stumpf R P, Putz F E and Workman T W 1999a Sea-level rise and coastal forest retreat on the west coast of Florida, USA *Ecology* **80** 2045–63

Williams K, Meads M V and Sauerbrey D A 1998 The roles of seedling salt tolerance and resprouting in forest zonation on the west coast of Florida, USA *Am. J. Bot.* **85** 1745–52

Williams K, Pinzon Z S, Stumpf R P and Raabe E A 1999b Sea-level rise and coastal forests on the Gulf of Mexico *US Geol. Surv.* **1500** 20910

Young R 1995 Coastal wetland dynamics in response to sea-level rise: transgression and erosion *Doctoral Dissertation* Duke University